JOURNAL OF Materials CHEMISTRY

Electrodeposition of silver selenide thin films from aqueous solutions

Ruizhi Chen, Dongsheng Xu, Guolin Guo* and Youqi Tang

State Key Laboratory for Structural Chemistry of Unstable and Stable Species, Institute of Physical Chemistry, Peking University, Beijing 100871, P. R. China.
E-mail: guogl@pku.edu.cn

Received 7th August 2001, Accepted 11th February 2002
First published as an Advance Article on the web 26th March 2002

Silver selenide thin films have been electrodeposited potentiostatically from aqueous acid solutions containing silver ions complexed with SCN^- and selenium dioxide at room temperature. The electrodeposition reactions were studied by cyclic voltammetry. The deposited films were characterized by X-ray diffraction (XRD), energy dispersive X-ray spectroscopy (EDS), X-ray photoelectron spectra (XPS) and scanning electron microscopy (SEM). The influence of deposition parameters such as potential, electrolyte composition and pH-value on the chemical composition and crystallinity of the films is discussed. The compositions of silver selenide films were controlled continuously from Ag-rich to near stoichiometry by adjusting the bath concentration and deposition potential. After annealing and slowly cooling in argon atmosphere, the films are highly (002) oriented. Furthermore, the excess Ag in the films transformed into Ag_2Se by annealing in Se vapor at 230 °C for 4–5 h.

Introduction

Silver selenide (Ag_2Se) is an $A_2^{I}B^{IV}$ group compound semiconductor. It undergoes a polymorphic-phase transition at 133 °C.[1] The low-temperature phase orthorhombic β-Ag_2Se is a narrow band gap semiconductor with an energy gap of *ca.* 0.07 eV.[2] Its high-temperature phase of cubic α-Ag_2Se shows the properties of a metal and is a well-known superionic conductor.[1,3] Silver selenide could be applied in various fields such as infrared sensors, photolithographic layers, electrochemical storage cells and electrochemical potential memory devices, *etc.*[4–7] Recently, Xu *et al.*[8] reported that non-stoichiometric $Ag_{2+\delta}Se$ shows a large, positive magnetoresistance (MR) effect. The significant MR of $Ag_{2+\delta}Se$ at room temperature and its linear dependence on magnetic fields could make it a promising material for technological application in magnetic field sensing devices,[9] especially applied to the low field sensors.

Bulk Ag_2Se was prepared traditionally by solid phase reaction of high-purity Ag and Se in a stoichiometric ratio.[1] Non-stoichiometric $Ag_{2+\delta}Se$ was obtained by heating the mixture of Ag_2Se and appropriate amounts of silver or selenium at above the melting point of Ag_2Se.[8] Thin films of Ag_2Se were deposited by the technique of vacuum evaporation of bulk Ag_2Se,[1] solid–vapor-phase reaction of evaporated silver and selenium,[10,11] and chemical bath deposition.[12,13] Among various film deposition strategies, electrodeposition is a cost-effective method for the fabrication of binary and ternary chalcogenide semiconductors[14] and has been successfully employed for the deposition of selenide semiconductors, *e.g.* ZnSe,[15] CdSe,[16] PbSe[17,18] and Bi_2Se_3.[19] However, preparation of Ag_2Se film by electrodeposition is more difficult than that of the above selenides due to the higher redox potential of Ag^+/Ag. Gobrecht *et al.*[20] first reported the electrodeposition of silver selenide from an H_2SeO_3 electrolyte (pH = 2) on a silver cathode. Thin layers of $Ag_{2+\delta}Se$ have been electrodeposited from strongly acidic electrolytes containing SeO_2 and $AgNO_3$.[21–24] Considerable over-stoichiometric Ag existed in the films, and the reported low limit of δ is 0.4[21] and *ca.* 0.2–0.3[23,24] for the films deposited on Pt or Au cathodes. The present paper is devoted to the electrodeposition of silver selenide films from an aqueous bath containing SeO_2, $AgNO_3$ and KSCN. SCN^- was introduced as a complexing ligand to lower the reduction activity of Ag^+. The film compositions were tuned continuously from Ag-rich to near stoichiometry by adjusting the bath composition and the deposition potential. Furthermore, the slight excess of Ag in the deposited film can be transformed into Ag_2Se by annealing in Se vapor.

Experimental

Silver selenide films were cathodically electrodeposited from solutions containing 0.5 M KSCN, 5.0 mM $AgNO_3$, 0.05 M KNO_3 and various concentrations of SeO_2, *i.e.* 2.0, 2.5 and 3.0 mM. Silver nitrate ($AgNO_3$, 99.9%) and selenium(IV) oxide (SeO_2, 99.8%, ACROS) were used without further purification. KSCN (AR) and KNO_3 (AR) were purified to remove some heavy metal impurities of Fe, Pb, Cu, *etc.* The purification process involved passing their solutions (about 500 g l^{-1} KSCN or 200 g l^{-1} KNO_3) through chromatographic columns containing blended active charcoal and 8-hydroxyquinoline, and then evaporation and recrystallization. The electrolyte solutions were made up with double distilled water. The pH-value of the solutions was adjusted to 2.6 using a *ca.* 1 : 15 (v : v) aqueous HNO_3 solution. At this pH SeO_2 is in the form of selenous acid ($HSeO_3^-$ and H_2SeO_3) in aqueous solutions. SCN^- was used to complex Ag^+ in order to prevent the precipitation of insoluble Ag_2SeO_3 and to decrease the redox potential of Ag^+/Ag.

Film electrodeposition was carried out using a three-electrode system with a saturated calomel electrode (SCE) as the reference electrode and a Pt plate as the counter electrode. The working electrode was an indium-doped tin oxide (ITO) covered glass with a sheet resistance of *ca.* 20 Ω cm. All potentials are expressed *versus* SCE. The ITO substrates were cleaned ultrasonically in 0.1 M NaOH, double distilled water, acetone and then rinsed in double distilled water. Cyclic voltammetry measurements were carried out using a CHI660A Potentiostat/Galvanostat (CH Instruments Inc., China). Both electrodepositon and cyclic voltammetry were carried out in unstirred solutions in a thermostatted cell (20 °C).

The as-deposited films were washed with double distilled water, and then dried in air at room temperature. Furthermore,

DOI: 10.1039/b107177g

the films were annealed by two different processes. One process is annealing in argon atmosphere at 200 °C for 80–90 min first and then cooling the films down slowly (*ca.* 1 °C min^{-1}) to room temperature in a tubular furnace. The other process is annealing in Se vapor. First, the film samples and a small amount of Se powder were placed into a glass tube, the tube was then evacuated and sealed, and then finally annealed at 230 °C for 4–5 h. In order to remove the remaining Se on the surface of the treated films during the cooling process, the films were dipped into hot DMSO (180–185 °C) for *ca.* 10 min, cooled down slowly and washed with alcohol.

The phase identification was characterized by X-ray diffraction (XRD), which was performed on a rotating anode Rigaku (Japan) X-ray diffractometer using Ni-filtered Cu Kα radiation. The X-ray tube was operated at 40 kV and 70 mA. Surface morphologies of the films were studied using an AMARY 1910FE scanning electron microscopy (SEM). Chemical compositions of the films were measured using an energy dispersive X-ray spectrometer (EDS) installed on JSM-6301F SEM equipment combined with an Oxford Link ISIS 300 analyzer (E = 10 keV). X-Ray photoelectron spectra (XPS) of the film were recorded on a VG-ESCALAB 5 using Al Kα as the exciting source. The anode was operated at 9 kV and 18.5 mA and the chamber pressure was kept at 10^{-8} Torr. The binding energies obtained in the XPS analysis were corrected for specimen charging using C 1s as the reference at 284.60 eV.

Results and discussion

1 Cyclic voltammetry and film electrodeposition reactions

Fig. 1(a) shows a scan of the solution containing 2.5 mM SeO_2 and 0.1 M KNO_3 at pH 2.60. During a cathodic scanning, the curve shows a small reduction wave for $HSeO_3^-$ to Se [eqn. (1)] at about −0.5 V followed by an increase of cathodic current which can be attributed to further reduction of Se to H_2Se [eqn (2)].[17,18] A reddish Se film was observed on the substrate after depositing at a constant potential of −0.5 V, and the XPS identification of the deposited film confirms the formation of Se. Below −1.2 V *vs.* SCE, hydrogen evolution commences. Direct, six-electron reduction of the $HSeO_3^-$ to H_2Se has also been reported.[25] The corresponding oxidation peaks of eqns. (2) and (1) can be seen at potentials of +0.42 and +0.95 V *vs.* SCE, respectively.

$$HSeO_3^-(aq) + 5H^+(aq) + 4e^- \rightarrow Se(s) + 3H_2O \quad (1)$$

$$Se(s) + 2H^+(aq) + 2e^- \rightarrow H_2Se(aq) \quad (2)$$

Fig. 1(b) presents the cyclic voltammogram of a solution containing 5.0 mM $AgNO_3$ complexed with 0.5 M KSCN. Silver deposition on the substrate is evident by the appearance of a cathodic peak at −0.32 V, which is stripped off during the backward sweep giving rise to an anodic peak at −0.05 V. Our experimental results indicated that the pH-value of the $Ag(SCN)_n^{1-n}$ ($2 \leqslant n \leqslant 4$) solution has little effect on the redox potential of Ag^+/Ag.

Cyclic voltammetry of a solution containing $Ag(SCN)_n^{1-n}$ and selenous acid is shown in Fig. 1(c). The reduction peak at −0.34 V is associated with the formation of Ag. The second peak at −0.47 V is due to the reduction of selenous acid to Se. The cathodic wave below −0.55 V is caused by the induced deposition of Ag_2Se due to the formation of insoluble Ag_2Se ($\log K_{sp} = -63.7$[26]) according to eqn. (3) or eqn. (4) proposed by Vittori and coworkers.[22]

$$2Ag(SCN)_n^{1-n} + Se + 2e^- \rightarrow Ag_2Se + 2nSCN^- \quad (3)$$

$$2Ag(SCN)_n^{1-n} + HSeO_3^- + 6e^- + 5H^+ \rightarrow Ag_2Se + 3H_2O + 2nSCN^- \quad (4)$$

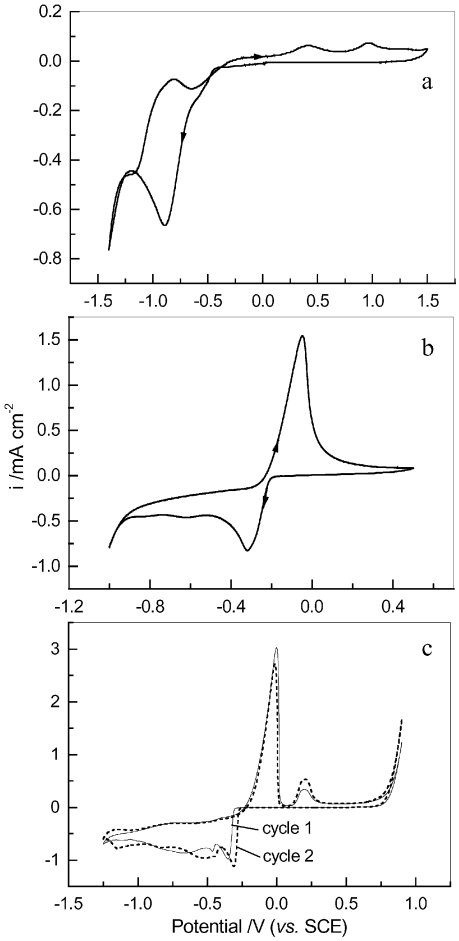

Fig. 1 Cyclic voltammogram for an ITO electrode in the plating solution containing: (a) 2.5 mM SeO_2 and 0.1 M KNO_3, pH 2.60; (b) 5.0 mM $AgNO_3$ complexed with 0.5 M KSCN; and (c) 0.5 M KSCN, 5.0 mM $AgNO_3$, 2.5 mM H_2SeO_3 and 0.05 M KNO_3, pH 2.60, solid line for the first scan and dotted line for the second scan. The scan rate in all three figures is 50 mV s^{-1}.

The dotted line in Fig. 1(c) shows the voltammogram for the second scan, that is, the working electrode was actually silver selenide instead of ITO. It can be seen that Ag_2Se deposited at a more positive potential than on the ITO surface. In the reversed scan the oxidation peak at a potential of *ca.* 0.0 V is due to the oxidation of silver. The second anodic wave which appeared at a potential of 0.2 V is characteristic for the oxidation of chemically bonded Se(II) from Ag_2Se [the reverse reaction of eqn. (3)]. The anodic wave at a potential above +0.9 V is due to the oxidation of selenium.

From the above cyclic voltammograms, Ag_2Se could be deposited at potentials of between −0.55 and −0.75 V *vs.* SCE. Meanwhile, the deposition would be accompanied by the formation of silver. The deposited silver can participate in electrode reaction and be transformed into Ag_2Se according to eqn. (5).[23,25]

$$2Ag + HSeO_3^- + 5H^+ + 4e^- \rightarrow Ag_2Se + 3H_2O \quad (5)$$

By adjusting the concentration of the Ag^I and Se^{IV} source and lowering the pH-value of the electrolyte, the potential of $HSeO_3^-$ to Se and Ag_2Se deposition would be shifted close to that of Ag^+ to Ag. On the other hand, by decreasing the deposition potential to an appropriate position, the deposition rate of Ag_2Se is increased and the reduction rate of Ag^+ to Ag is decreased. Therefore, near-stoichiometric Ag_2Se films are expected to be obtained.

2 Film characterization and effect of deposition parameters

Silver selenide thin films were deposited at potentials between −0.60 and −0.75 V *vs.* SCE from electrolytes containing fixed concentrations of $AgNO_3$, KSCN and KNO_3 and various selenous concentrations, of 2.0, 2.5 and 3.0 mM. The current densities during the deposition stabilized within a minute after the start of the plating and remained relatively constant in the range of −0.25 to −0.33 mA cm^{-2}. The deposition time was kept constant at 40 min. EDS, XRD, XPS and SEM were used to reveal the nature of the films.

The chemical compositions of the films were determined by quantitative analyses of the EDS spectra. The EDS data were collected on an area of *ca.* 14 × 8 μm. Fig. 2(a) shows a typical EDS spectrum of the film deposited at a potential of −0.70 V *vs.* SCE from the electrolyte with a concentration ratio of $Ag(SCN)_n^{1-n}$: SeO_2 of 5.0 mM : 2.5 mM, in which only the peaks of Se and Ag appeared. Quantitative analysis shows that the atomic ratio of Ag : Se is 66.5 : 33.5, which gives a near-stoichiometric composition. Furthermore, the composition analysis results of the films deposited from different selenous acid concentrations at potentials between −0.60 and −0.75 V are listed in Table 1. The relative error of atomic ratio measured by EDS is within 3% limited by the instrument. As seen from Table 1, the deposition potential and the electrolyte concentration apparently affect the film compositions. For example, when the concentration ratio of $Ag(SCN)_n^{1-n}$: SeO_2 is 5.0 mM : 2.5 mM, the Ag : Se ratios of the deposited films tend toward stoichiometry with lowering the potential from −0.60 to −0.70 V.

Table 1 Atomic ratios (Ag : Se) of the films electrodeposited under different conditions measured by EDS

	Electrolyte composition		
	$[Ag(SCN)_n^{1-n}]$: $[SeO_2]$ (mM : mM)		
Potential/V *vs.* SCE	5.0 : 2.0	5.0 : 2.5	5.0 : 3.0
−0.60	3.2	2.6	2.5
−0.65	2.6	2.2	2.1
−0.70	2.4	2.0	2.2
−0.75	3.2	3.0	2.7

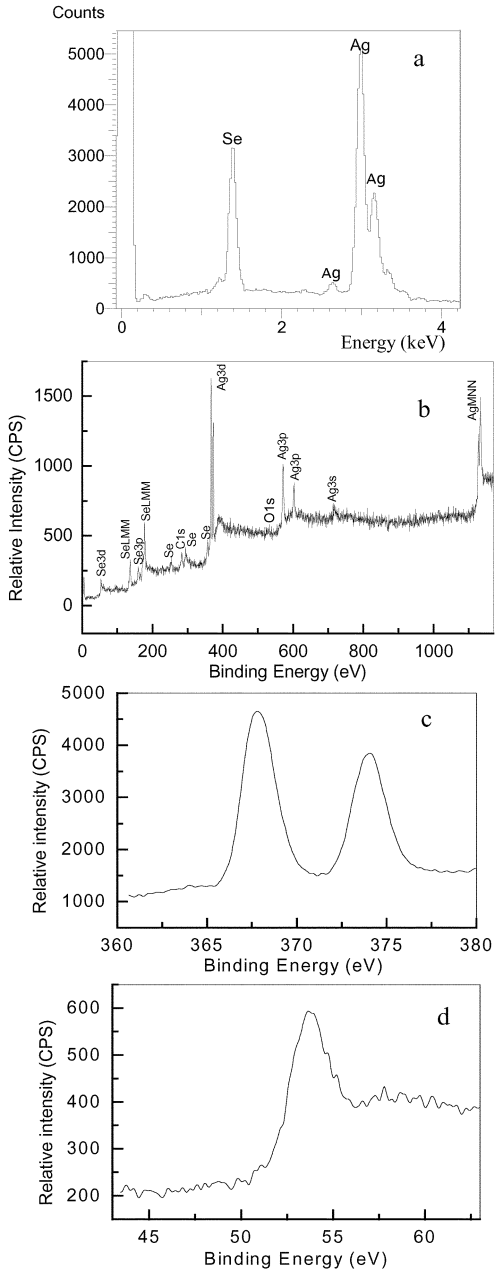

Fig. 2 Typical EDS spectrum (a), XPS survey spectrum (b), Ag 3d spectrum (c) and Se 3d spectrum (d) of the film deposited from solution containing 0.5 M KSCN, 5.0 mM $AgNO_3$, 0.05 M KNO_3, and 2.5 mM SeO_2, pH 2.60 at a potential of −0.70 V *vs.* SCE.

Fig. 2(b) presents the XPS survey spectrum of the as-deposited film corresponding to the sample in Fig. 2(a). All the peaks were identified and attributed to Se, Ag, C and O. The presence of carbon and oxygen was attributed to the atmospheric exposure of the film. No impurity peaks were detected, such as S 2p of Ag_2S (160.8 eV[27]) originating from reduction of SCN^-, Se 3d of SeO_2 (59.8 eV[28]), *etc.* Accurate binding energies (E_b) were obtained by repeatedly scanning over narrow energy ranges containing the peaks and measuring at the mid-waves. The narrow spectra of Ag 3d and Se 3d are shown in Fig. 2(c) and (d). The E_b values for Se $3d_{5/2}$ and Ag $3d_{5/2}$ are 53.3 and 367.9 eV, respectively. In addition, the Ag Auger parameter α is 718.8 eV, which was determined by Ag $3d_{5/2}$ and $AgM_4N_{45}N_{45}$ (1135.7 eV) according to

$$\text{Auger } \alpha/\text{eV} = \text{AlK}\alpha\ (1486.6\ \text{eV}) - \text{AgMNN} + \text{Ag } 3d_{5/2}$$

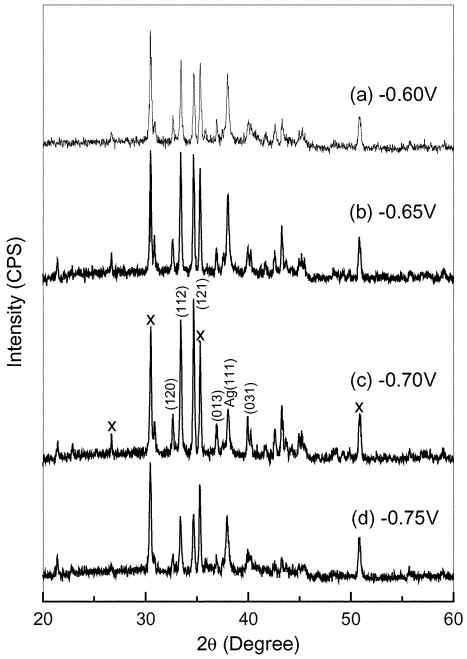

Fig. 3 XRD patterns of the films deposited at different potentials: (a) −0.60 V, (b) −0.65 V, (c) −0.70 V, (d) −0.75 V. Plating bath: 0.5 M KSCN, 5.0 mM $AgNO_3$, 0.05 M KNO_3, 2.5 mM SeO_2 and pH 2.60. × for ITO diffraction peaks.

These values are very close to the E_b values reported for Ag_2Se (Se $3d_{5/2}$ = 53.8 eV,[29] Ag $3d_{5/2}$ = 367.8 eV and Auger α = 719.2 eV[30]), and deviate from the standard values in elemental Se (Se $3d_{5/2}$ = 55.9 eV[31]) and Ag (Ag $3d_{5/2}$ = 368.3, Auger α = 720.2 eV[30]). Thus, it can be concluded that the as-deposited film is mainly composed of compound Ag_2Se.

Fig. 3 shows XRD patterns of the films deposited at different potentials, when the concentration ratio of $Ag(SCN)_n^{1-n}$: SeO_2 is 5.0 mM : 2.5 mM. The characteristic X-ray diffraction patterns further confirmed the formation of the Ag_2Se compound. The diffraction peaks [see Fig. 3(c)] at 2θ = 32.67, 33.43, 34.67 and 36.96°, *etc.*, can be indexed to (120), (112), (121) and (013) of orthorhombic β-Ag_2Se (space group $P2_12_12_1$), respectively. The peak positions and the relative intensities are in agreement with the standard powder diffraction data (JCPDS No. 24-1041). Apart from the Ag_2Se phase, the excess Ag (111) diffraction peak was detected. The relative intensity of Ag (111) compared with Ag_2Se (112) and (121) decreases with lowering the deposition potential from −0.60 to −0.70 V, which is consistent with the EDS results. For the films deposited at potentials more negative than −0.70 V, a decrease of the intensities of Ag_2Se diffraction peaks is observed, as well as an increase of the Ag (111) peak.

In addition, the films deposited at potentials between −0.60 and −0.70 V for three bath compositions are dark grey in color and adhere strongly to the substrates. However, the film deposited at a potential of −0.75 V is rough and exhibits poor adhesion. At potentials more negative than −0.75 V, most of the products precipitate into the solution instead of adhering to the substrate. It can be explained that, at sufficiently negative potentials, a soluble compound H_2Se, formed *via* eqn. (2),[15] diffuses into the solution and reacts with silver ions to produce the precipitation of Ag_2Se in solution by eqn. (6), instead of the electrodeposition of Ag_2Se by eqns. (3) and (4).

$$2\,Ag^+ + H_2Se \rightarrow Ag_2Se + 2\,H^+ \qquad (6)$$

In order to get a uniform and well adhering film, the solution should contain low concentrations of Ag^+ and SeO_2 and be unstirred. To lower the reduction activity of Ag^+, a higher concentration of 0.5 M SCN^- was used. As seen from Table 1, at the fixed potentials the Ag : Se atomic ratios tend toward stoichiometry with increasing the selenous acid concentration from 2.0 to 2.5 mM. When its concentration is increased to 3.0 mM, the film compositions have less improvement, even the Ag : Se ratio deviates from stoichiometry at a potential of −0.70 V. The optimal deposition potential moves to a more positive value, −0.65 V, which corresponds to the atomic ratio of Ag : Se = 67.7 : 32.3.

The pH-value of the solutions also affects the composition of the deposited films. As expressed by eqn. (1) and (2), a lower pH of the solution results in a more positive redox potential of $HSeO_3^-$/Se, and further reduction of Se to H_2Se, or $6e^-$ reduction of $HSeO_3^-$ to H_2Se. On the other hand, a lower pH can also facilitate the induced deposition of insoluble Ag_2Se as expressed by eqns. (4) and (5). The natural pH of the mixed solution is *ca.* 3.15 at a selenous acid concentration of 2.5 mM. In our experiments, the appropriate deposition potential is −0.70 V at a solution pH of 2.60. If the pH-value continues to be lowered, the optimal deposition potential would move to a more positive position.

3 Effect of annealing

To improve the crystallinity, the films were annealed in an Ar atmosphere at 200 °C. Fig. 4(a) shows the XRD pattern of the annealed film corresponding to the sample in Fig. 3(c). It is quite different from that of the as-deposited film shown in Fig. 3(c). For the Ag_2Se phase, only the (002) and (004) diffraction peaks were observed at 2θ = 22.90 and 46.79°,

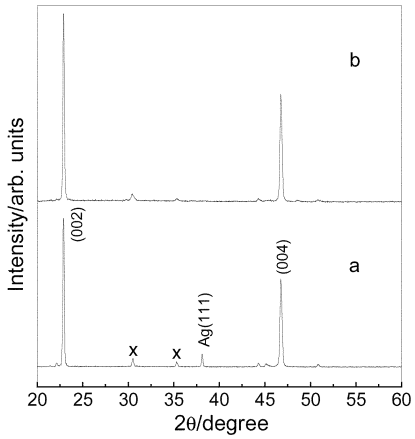

Fig. 4 XRD patterns of the annealed Ag_2Se films corresponding to the sample in Fig. 3(c): (a) annealed at 200 °C in Ar atmosphere for 90 min; (b) annealed in Se vapor at 230 °C for 5 h. × for ITO diffraction peaks.

respectively. The contribution of other primary diffraction planes, (112) and (121), are completely suppressed in comparison with that of the polycrystalline orthorhombic Ag_2Se standard, in which the intensity ratio between (002) and (112) is 6 : 100. The strong intensities of (002) and (004) indicate that the annealed silver selenide film is (002) highly oriented along the direction parallel to the film plane. The oriented Ag_2Se film was only formed by slow cooling during the phase transformation from the high-temperature cubic phase to the low-temperature orthorhombic phase. With fast cooling, no (002) oriented film was formed. For example, if the film sample was quenched at 160 °C, the polycrystalline Ag_2Se phase developed, which is consistent with the reported result.[11] Sáfrán *et al.*[11] supposed that the enthalpy difference between the high-temperature and low-temperature phases and the low surface energy of the (001) Ag_2Se is the driving force of (002) orientation. As seen from Fig. 4(a), the Ag (111) peak was still detected in the XRD pattern, which implies that a slight excess of Ag still exists in the film. In order to decrease the excess Ag and prepare stoichiometric Ag_2Se, the films were annealed in Se vapor. After annealing at 230 °C for 5 h, the Ag (111) diffraction peak completely disappeared from the XRD pattern [Fig. 4(b)]. Even for the film deposited at −0.60 V, the Ag (111) peak was not observed after annealing in Se vapor.

Fig. 5(a)–(c) shows the typical SEM surface morphologies of the films deposited at various potentials. It can be shown that the average grain size decreases with lowering the deposition potential. Fig. 5(b) shows that the as-deposited Ag_2Se film at −0.70 V consists of crystalline grains with diameters of *ca.* 300–500 nm. The SEM image of the film after annealing in Ar shows a difference in the morphology and grain size. The crystalline grains become globular and the diameters are in the range of 500–800 nm, which are larger than the crystallites of the corresponding as-deposited film [Fig. 5(b)].

Conclusions

Using the technique of potentiostatic electrodeposition, nearly stoichiometric polycrystalline Ag_2Se films were deposited from 0.5 M KSCN, 5.0 mM $AgNO_3$, 2.5 mM SeO_2 and 0.05 M KNO_3 at a potential of −0.70 V *vs.* SCE at room temperature. The films deposited under this condition are mirror-like with a dark greyish color and well-adhering to the substrates. To obtain nearly stoichiometric Ag_2Se, the permitted range of deposition parameters including bath composition, pH and deposition potential are rather limited, which arise from the accompanying side electrochemical reactions of Ag and Se with Ag_2Se electrodeposition. The Ag_2Se films with Ag over-stoichiometry can be deposited from electrolytes containing

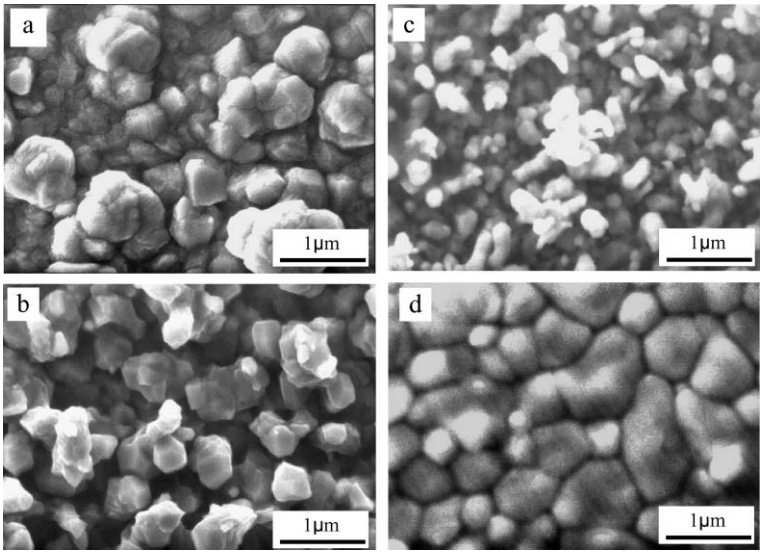

Fig. 5 Top view SEM images of the as-deposited Ag_2Se films obtained at potentials of: (a) −0.60 V, (b) −0.70 V, and (c) −0.75 V *vs.* SCE, and the annealed film (d) corresponding to (b). Plating bath: 0.5 M KSCN, 5.0 mM $AgNO_3$, 0.05 M KNO_3, 2.5 mM SeO_2 and pH 2.60.

low concentrations of Ag^+ and SeO_2, between potentials of −0.60 and −0.70 V *vs.* SCE. The ratio of Ag : Se can be tuned continuously from *ca.* 3.0 to 2.0 by adjusting the electrolyte composition and the deposition potential. After annealing in an Ar atmosphere, the (002) oriented Ag_2Se films were developed. In addition, stoichiometric Ag_2Se films can be obtained under electrolyte compositions and deposition potentials over a wide range using the method of annealing in Se vapor.

Acknowledgements

This work was supported by the Major State Basic Research Development Program (Grant No. 2000077503).

References

1 V. Damodara Das and D. Karunakaran, *J. Appl. Phys.*, 1990, **68**, 2105.
2 R. Dalven and R. Gill, *Phys. Rev.*, 1967, **159**, 645.
3 P. Junod, *Helv. Phys. Acta*, 1958, **32**, 567.
4 C. Y. Liang and K. Tada, *J. Appl. Phys.*, 1988, **64**, 4494.
5 R. G. Lope and H. J. Goldsmit, *J. Appl. Phys.*, 1995, **16**, 1501.
6 K. Somogyi and G. Sáfrán, *J. Appl. Phys.*, 1995, **78**, 6855.
7 T. Okabe and K. Ura, *J. Appl. Crystallogr.*, 1993, **27**, 140.
8 R. Xu, A. Husmann, T. F. Rosenbaum and M. L. Saboungi, *Nature (London)*, 1997, **390**, 57.
9 G. A. Prinz, *Science*, 1998, **282**, 1660.
10 R. P. Sharma, *Indian J. Pure Appl. Phys.*, 1997, **35**, 424.
11 G. Sáfrán, L. Malicskó, O. Geszti and G. Radnóczi, *J. Cryst. Growth*, 1999, **205**, 153.
12 K. C. Sharma, R. P. Sharma and J. C. Garg, *Indian J. Pure Appl. Phys.*, 1990, **28**, 546.
13 B. Pejova, M. Najdoski, G. Ivan and K. Dey Sandwip, *Mater. Lett.*, 2000, **43**, 269.
14 C. D. Lokhande and S. H. Pawar, *Phys. Status Solidi A*, 1989, **111**, 17.
15 C. Natarajan, M. Sharon, C. Lévy-Clément and M. Neumann-Spallart, *Thin Solid Films*, 1994, **237**, 118.
16 G. J. Houston, J. F. Mccann and D. Henemann, *J. Electrochem. Soc.*, 1982, **129**, 37.
17 H. Saloniemi, T. Kanniainen, M. Ritala, M. Leskela and R. Lappalainen, *J. Mater. Chem.*, 1998, **8**, 651.
18 A. N. Molin and A. I. Dikusar, *Thin Solid Films*, 1995, **265**, 3.
19 A. P. Torane, C. D. Lokhande, P. S. Patil and C. H. Bhosale, *Mater. Chem. Phys.*, 1998, **55**, 51.
20 H. Gobrecht, H. D. Liess and A. Tausend, *Ber. Bunsen-Ges. Phys. Chem.*, 1963, **67**, 930.
21 E. Pacauskas, J. Janickis and I. Lasaviciene, *Liet. TSR Mokslu Akad. Darb., Ser. B*, 1971, **2**, 61.
22 M. David, R. Modolo, M. Traore and O. Vittori, *Electrochim. Acta*, 1986, **31**, 851.
23 M. T. Neshkova, V. D. Nikolova and V. Petrov, *J. Electroanal. Chem.*, 2000, **487**, 100.
24 M. T. Neshkova and E. Pancheva, *Anal. Chim. Acta*, 1991, **242**, 73.
25 M. S. Kazacos and B. Miller, *J. Electrochem. Soc.*, 1980, **127**, 869.
26 M. C. Mebra and A. O. Gubeli, *Can. J. Chem.*, 1970, **84**, 3491.
27 V. Kumar Kaushik, *J. Electron Spectrosc. Relat. Phemon.*, 1991, **56**, 273.
28 M. Shenasa, S. Sainkar and D. Lichtman, *J. Electron Spectrosc. Relat. Phemon.*, 1986, **40**, 329.
29 S. Zembutsu, *Appl. Phys. Lett.*, 1981, **39**, 969.
30 R. Romand, M. Roubin and J. P. Deloume, *J. Electron Spectrosc. Relat. Phenom.*, 1978, **13**, 229.
31 A. B. Mandale, S. Badrinarayanan, S. K. Datem and A. P. B. Sinha, *J. Electron Spectrosc. Relat. Phenom.*, 1984, **33**, 61.